Magnetic Dipole Scattering from Metallic Nanowire for Ultrasensitive Deflection Sensing

Xi, Zheng; Urbach, H. P.

DOI
10.1103/PhysRevLett.119.053902

Publication date
2017

Document Version
Final published version

Published in
Physical Review Letters

Magnetic Dipole Scattering from Metallic Nanowire for Ultrasensitive Deflection Sensing

Zheng Xi* and H. P. Urbach
Optics Reseach Group, Delft University of Technology, Department of Imaging Physics, Lorentzweg 1, 2628CJ Delft, The Netherlands
(Received 13 April 2017; published 1 August 2017)

It is generally believed that when a single metallic nanowire is sufficiently small, it scatters like a point electric dipole. We show theoretically when a metallic nanowire is placed inside specially designed beams, the magnetic dipole contribution along with the electric dipole resonance can lead to unidirectional scattering in the far field, fulfilling Kerker's condition. Remarkably, this far-field unidirectional scattering encodes information that is highly dependent on the nanowire's deflection at a scale much smaller than the wavelength. The special roles of small but essential magnetic response along with the plasmonic resonance are highlighted for this extreme sensitivity as compared with the dielectric counterpart. In addition, the same essential role of the magnetic dipole contribution is also presented for a very small metallic nanosphere.

DOI: 10.1103/PhysRevLett.119.053902

The scattering of light by nanoparticles has attracted significant attention from a fundamental point of view [1–3]. In particular, it is interesting to study the interaction of specially designed *magnetic atoms* with the often neglected magnetic field component of light [4–18]. This magnetic interaction has led to many fascinating phenomena, such as superlensing, cloaking, negative refraction, and directional scattering. However, for a simple metallic nanostructure like a nanosphere or a nanowire (with cross section) much smaller than the wavelength, this magnetic response is several orders of magnitude weaker, while its electric counterpart still shows large enhancement due to localized plasmonic resonance (LPR). Because of this, the scattering of light as an electromagnetic wave becomes the scattering of an electric field by an electric dipole instead.

Despite its simple geometry, the scattering by a nanowire still shows its important role in fields such as optomechanics, atomic force microscopy, and quantum mechanical measurement [19–24]. The far-field optical deflection measurement of the nanowire based on scattering has greatly enhanced our ability to investigate imaging and dynamics at length scales much smaller than the wavelength. The nanowire, in this case, is treated as a nonresonant electric dipole scatterer, with a symmetric far-field scattering pattern [20]. The resulting change in the far field for small deflections is not high, which sets a limiting factor on the sensitivity of the scheme.

In this Letter, we report the essential role of the magnetic response of a metallic nanowire much smaller than the wavelength, especially at LPR frequency, in developing a method to measure the nanowire's deflection with ultrahigh sensitivity. Specifically, we consider the scattering of a metallic nanowire inside specially designed beams rigorously using Mie theory. By moving the metallic nanowire around the point where the magnetic field is maximum with minimum electric field, we found that directional far-field scattering can be achieved even for a single metallic nanowire, fulfilling Kerker's condition [25]. The highly directional far-field scattering encodes information about the nanowire's deflection with extreme sensitivity [26,27]. The enhanced sensitivity compared with the high refractive index (HRI) material counterpart is discussed in detail. The present scheme can also by applied to a metallic nanosphere much smaller than the wavelength.

The considered geometry is sketched in Fig. 1(a). A silver nanowire of radius $R = 10$ nm (only the cross section is shown) is placed within four orthogonally oriented TE beams of equal intensity (the magnetic field is polarized along the z axis). The center position of the nanowire is described by $\mathbf{r_0} = (r_0, \theta_0)$ in polar coordinates. The phases of the four beams are chosen such that the H_z component is maximum at the origin. This geometry has been extensively used to trap and manipulate atoms in an optical lattice [28–30] and can be implemented using the common dark-field illumination

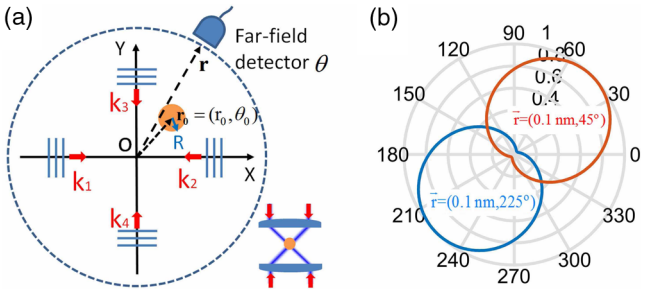

FIG. 1. (a) Geometry of the system. The nanowire of radius R (gold cross section) is displaced from the origin O by $\mathbf{r_0} = (r_0, \theta_0)$. Four incoming beams k_1 to k_4 intersect at O with constructive interference for H_z at this point. The far-field detector at $\mathbf{r}$ collects the scattered far field along the θ direction. The bottom illustration shows the schematic implementation with 4Pi illumination with cylindrical lenses. (b) Far-field scattering power pattern in the XY plane when the deflection is $\mathbf{r_0} = (0.1\ \text{nm}, 45°)$ (red curve) and $\mathbf{r_0} = (0.1\ \text{nm}, 225°)$ (blue curve).

scheme shown at the bottom of Fig. 1(a). The silver nanowire is placed in vacuum and it exhibits a LPR at $\lambda = 337$ nm [31] under the quasistatic approximation [2]. Figure 1(b) shows the far-field scattering pattern at this wavelength when the nanowire is displaced from the center origin O by $\mathbf{r_0} = (0.1\ \text{nm}, 45°)$ and $\mathbf{r_0} = (0.1\ \text{nm}, 225°)$. The silver nanowire in this case no longer scatters like an electric dipole, but with a highly asymmetric pattern when it is away from the origin O. The scattered power always reaches its maximum along the deflection direction $\theta = \theta_0$, and it has its minimum in the opposite direction $\theta = \theta_0 + \pi$. For the opposite deflection directions, the maximum and minimum switch, even for $r_0 = 0.1$ nm.

In order to understand this phenomenon, a theoretical model based on Mie theory to calculate the far-field scattering at the detector placed at $\mathbf{r}$ is developed. In the original Mie scattering theory, only one incident plane wave is considered and the corresponding far field can be calculated as [3]

$$H_{z,\text{Mie}}(\mathbf{r}) = -4iG_0\left(a_0 + 2\sum_{n=1}^{\infty} a_n \cos(n\theta)\right), \quad (1)$$

where the terms a_n are the Mie coefficients which contain information about the scatterer, with a_0, a_1, and a_2 describing the induced magnetic dipole moment, electric dipole moment, and electric quadrupole moment, respectively, and other a_n for higher order multipole terms [3,32]. The scalar 2D Green function $G_0 = (i/4)H_0^{(1)}(k_0 r)$ is used, where $H_0^{(1)}(k_0 r)$ is the zeroth order Hankel function of the first kind and k_0 is the wave number in free space.

In our case, rotations for the four beams are required and the final scattering field can be added, which is

$$H_{z,\text{far}}(\mathbf{r}) = -\sum_{p=1}^{4} 4iG_0\left\{a_0 + 2\sum_{n=1}^{\infty} a_n \cos(n\theta_p)\right\} e^{i\mathbf{k_p}\cdot\mathbf{r}}. \quad (2)$$

θ_p is the relative incident angle of the four beams and the term $e^{i\mathbf{k_p}\cdot\mathbf{r}}$ is the extra phase gained by the displacement $\mathbf{r} = (r_0, \theta_0)$ for different beams. In the calculation, we fix the origin of the nanowire at the origin of the coordinate system and treat the displacement as extra phases for each incident beam. The correctness of the theoretical method is checked by numerical simulation using the finite element method [33].

Keeping the first three a_n terms, the scattered far field H_z along the θ direction is

$$\begin{aligned} H_{z,\text{far}}(\theta) = -4iG_0[&2a_0\cos(k_0 r_0\cos\theta_0) + 4ia_1\cos\theta\sin(k_0 r_0\cos\theta_0) + 4a_2\cos(2\theta)\cos(k_0 r_0\cos\theta_0) \\ &+ 2a_0\cos(k_0 r_0\sin\theta_0) + 4ia_1\sin\theta\sin(k_0 r_0\sin\theta_0) - 4a_2\cos(2\theta)\cos(k_0 r_0\sin\theta_0)]. \end{aligned} \quad (3)$$

For a displacement r_0 much smaller than the wavelength, i.e., $k_0 r_0 \ll 1$, we arrive at the final expression for the scattered far field:

$$H_{z,\text{far}}(\theta) = -16iG_0[a_0 + ia_1 k_0 r_0\cos(\theta - \theta_0)]. \quad (4)$$

Looking at this equation, the far-field contribution from the electric dipole a_1 is reduced because $k_0 r_0 \ll 1$; thus, the contribution of the magnetic dipole a_0 becomes more important. It is interesting to note that although the first three Mie coefficients are considered, only the first two dipolar terms play important roles here. The term a_2, which corresponds to the contribution of the electric quadrupole, cancels out in the above expression. This would allow the current analysis to be applied to larger radii as well. In the directions of $\theta = \theta_0$ and $\theta = \theta_0 + \pi$, the cosine term equals 1 and -1 such that the far fields in these two directions take the values

$$\begin{aligned} H_{z,\text{far}}(\theta = \theta_0) &= -16iG_0(a_0 + ia_1 k_0 r_0), \\ H_{z,\text{far}}(\theta = \theta_0 + \pi) &= -16iG_0(a_0 - ia_1 k_0 r_0). \end{aligned} \quad (5)$$

If the nanowire can be designed such that for a certain displacement r_0, $a_0 = ia_1 k_0 r_0$, then

$$\begin{aligned} H_{z,\text{far}}(\theta = \theta_0) &= -32iG_0 a_1 k_0 r_0, \\ H_{z,\text{far}}(\theta = \theta_0 + \pi) &= 0. \end{aligned} \quad (6)$$

In this case, the field in one direction is zero and in the other direction is maximal. A strong asymmetry is observed in the far field, as shown in Fig. 1(b). The expression

$$a_0 = ia_1 k_0 r_0 \quad (7)$$

gives the condition for maximum asymmetry in the far field.

Generally, the calculation of a_0 and a_1 involves Bessel functions and Hankel functions, which lacks a clear physical interpretation. However, when the radius R of the nanowire is much smaller than the wavelength of light, the following approximations can be made [1]:

$$\begin{aligned} a_0 &\approx -i\pi k_0^4 R^4 \frac{\epsilon - 1}{32}, \\ a_1 &\approx -i\pi k_0^2 R^2 \frac{\epsilon - 1}{4(\epsilon + 1)}, \end{aligned} \quad (8)$$

with their ratio

$$\frac{a_1}{a_0} \approx \frac{8}{k_0^2 R^2(\epsilon + 1)}. \quad (9)$$

$\epsilon = \epsilon' + i\epsilon''$ is the permittivity of the nanowire's material. For an infinitesimally thin metallic nanowire, the contribution from the magnetic dipole moment a_0 is considered to be a high order term $k_0^4 R^4$ as compared with the electric dipole a_1 under plane wave excitation, and thus is generally neglected. The far-field scattering resembles the one produced by the electric dipole. However, the denominator in a_1 indicates a LPR when $\epsilon' = -1$, or, more generally, a Fröhlich resonance [1]. At this wavelength, the ratio between a_1 and a_0 becomes purely imaginary and this fulfills the requirement by Eq. (7), which leads to

$$r_0 = \frac{\pi R^2 \epsilon_p''}{4\lambda_p}, \tag{10}$$

where λ_p is the LPR wavelength and ϵ_p'' is the imaginary part of the permittivity at resonance. A sharp asymmetry in the far field can be observed when the nanowire is at position r_0. This asymmetric far-field pattern cannot be produced by an electric dipole alone; it can only be observed when the magnetic contribution from the metallic nanowire is taken into account and optimized appropriately. Considering the value for the silver nanowire, $\lambda_p \approx 337$ nm, $R = 10$ nm, and $\epsilon_p'' \approx 0.58$ [31], a displacement of $r_0 \approx 0.1$ nm can lead to strong asymmetry in the far field, which explains the extreme sensitivity in Fig. 1(b). This rigorous treatment provides an accurate model for deducing very small deflections r_0 of the nanowire by measuring the asymmetry in the far field. Conversely, it also serves as a design guideline for choosing the nanowire's property for optimal sensing for a certain deflection r_0: for the measurement of smaller r_0, a smaller radius R, a smaller imaginary part ϵ_p'', and a longer resonance wavelength λ_p are preferred. What is interesting to note here is the inverse proportionality of r_0 to the resonance wavelength λ_p. For a recently highlighted material, indium tin oxide [34], the resonance is at $\lambda_p = 1.42$ μm, with $\epsilon_p'' \approx 0.5$ similar to silver. According to Eq. (9), a radius the same as for the silver case leads to an r_0 that is about 4 times smaller, but at infrared wavelength. The general condition for Fröhlich resonance allows us to explore materials involving surface phonon resonance, such as SiC [35]. The highly tunable plasmonic resonance in heavily doped semiconductor or core-shell materials also enriches the flexibility of the present scheme [1].

We would like to briefly discuss the cases for a nanowire made of a perfect electric conductor and a nanowire made of a purely dielectric material (real ϵ). For a perfect electric conductor ($\epsilon = -\infty$), the coefficients a_0 and a_1 are out of phase. For the purely dielectric case, a_0 and a_1 are in phase. The lack of $\pi/2$ phase difference as required by Eq. (6) in these two cases largely prevents the strong asymmetric far-field scattering.

Although the above analysis is based on the quasistatic approximation, the condition for maximum asymmetry given by Eq. (6) is rigorous for a larger radius R, as long as only the first three Mie coefficients dominate. A closer review of Eq. (6) reveals the general condition for maximum asymmetry at r_0: (1) The electric dipole contribution a_1 should be much larger than the magnetic dipole contribution a_0 for $k_0 r_0 \ll 1$ and (2) there should be a $\pi/2$ phase difference between them. This happens near the plasmonic resonance for metal or near the electric dipole resonance for HRI dielectric materials. A very strong asymmetry can also be expected around the *magnetic anapole mode*, where a_0 is nearly zero [36]. It is important to emphasize the role of the magnetic dipole contribution a_0 here, because without it, according to Eq. (4), the far field would be symmetric.

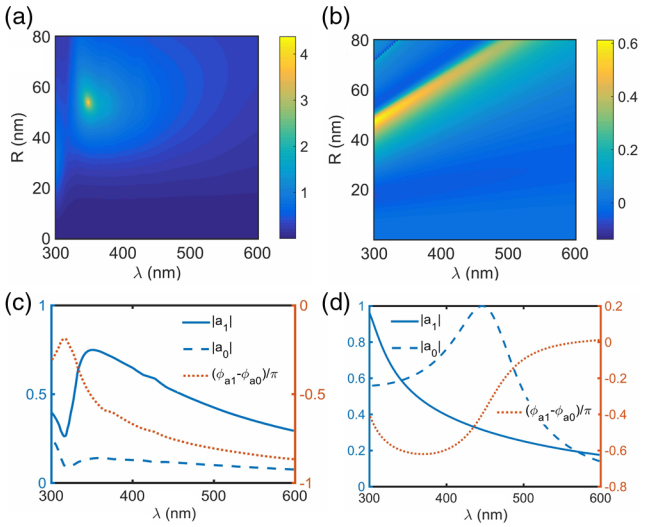

FIG. 2. (a) Plot of the sensitivity S for a silver nanowire for a displacement of 10 nm. (b) The same as (a) but for a HRI dielectric nanowire. (c) The contribution from the electric dipole coefficient a_1, the magnetic dipole coefficient a_0, and their phase difference for a silver nanowire of radius $R = 54$ nm. (d) The same as (c) but for a HRI dielectric nanowire of radius $R = 47$ nm.

To study this effect in more detail, we optimize the radius and working wavelength of the nanowire to achieve maximum sensitivity for a displacement measurement of 10 nm using the above rigorous treatment. We take the logarithmic power ratio in opposite directions,

$$S = \log_{10}\left|\frac{H_{z,\mathrm{far}}(\theta = \theta_0 + \pi)}{H_{z,\mathrm{far}}(\theta = \theta_0)}\right|^2, \tag{11}$$

to quantify the sensitivity. The results are shown in Figs. 2(a) and 2(b) for the case of a silver nanowire and an HRI dielectric nanowire with refractive index $n = 3.5$.

A clear difference can be seen between the two cases: for silver, a very large asymmetry of $S = 4.4$ can be observed at 348 nm for the radius $R = 54$ nm, whereas for the HRI dielectric case, only a moderate asymmetry of $S = 0.6$ can be observed at 300 nm when $R = 47$ nm.

In order to explain the difference between these two cases, we plot the absolute values of a_0, a_1, and their phase difference in Figs. 2(c) and 2(d), corresponding to the

radius R for which the maximum S is achieved. We are interested in the wavelength where the two coefficients have $\pi/2$ phase difference as required by Eq. (6). For silver, this happens at 348 nm, which corresponds to the LPR as indicated by a peak in $|a_1|$. Because there is no magnetic resonance for a silver nanowire, the ratio $|a_1|/|a_0|$ can be large, about 5 in this case. Substituting this into Eq. (6) would yield the displacement with the highest sensitivity at $r_0 = 10$ nm, which explains why S is so high at this point in Fig. 2(a). For the HRI dielectric case, in contrast with silver, there is an additional magnetic resonance for $|a_0|$ peaking at 435 nm besides the electric dipole resonance for $|a_1|$ peaking at 292 nm (not shown). Because of these two resonances, there are two wavelengths at which the two coefficients have $\pi/2$ phase difference, namely, at 311 and 428 nm, respectively. Only the first wavelength is of interest because we are looking for a large $|a_1|/|a_0|$. However, at this wavelength, the tail of the $|a_0|$ resonance is still high and thus $|a_1|/|a_0|$ decreased to about 1.4. Therefore, S is only 0.6, which is much lower than the metal case. It is expected that a large asymmetry occurs at a displacement r_0 of 34 nm to match $|a_1|/|a_0|$ in the HRI nanowire. It is interesting to note that if we move the nanowire around the maxima of the electric field E, then the second wavelength can be used [26]. However, as pointed out above, the strong overlap between the two resonances decreases the ratio between the two coefficients and, thus, sets a limit to the minimum r_0 that can be sensed using HRI for strong asymmetrical scattering compared with the metal case [26]. We have also discussed two aspects that are important for implementing this scheme into practice: namely, the amount of the scattered power and the shape of the nanowire. The detailed discussions can be found in the Supplemental Material [33].

Next, we extend the discussion to the 3D nanosphere case. The geometry of the 3D problem is the same as shown in Fig. 1(a) except that the nanowire is now replaced by a nanosphere with radius R. The scattered far field in the XY plane for each plane wave can be described by the phase function $S_2(\theta)$ [1]:

$$S_2(\theta) = \sum_{n=1} \frac{2n+1}{n(n+1)} (a_n \tau_n + b_n \pi_n), \tag{12}$$

where the terms a_n and b_n correspond to the contributions from the induced electric and magnetic multipoles. τ_n and π_n are terms describing the angular distribution of the scattered field.

For the calculation of the four beams case, a similar procedure as in the nanowire case can be applied [33]. Without going into detail, we arrive at the final expression for the displacement with the maximum asymmetry in the far field:

$$r_0 = \frac{2\pi R^2 \epsilon_p''}{15\lambda_p}, \tag{13}$$

with the condition $2b_1 = ia_1 k_0 r_0$ being satisfied.

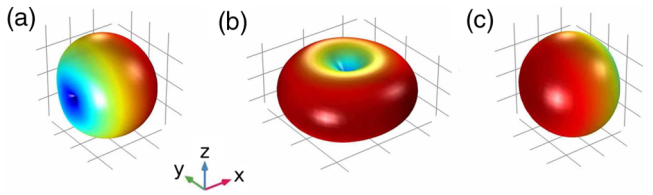

FIG. 3. Far-field scattering power pattern when a silver nanosphere of radius $R = 10$ nm is displaced from the origin along the X axis by (a) $r_0 = 0.07$ nm, (b) $r_0 = 0$ nm, and (c) $r_0 = -0.07$ nm at $\lambda_p = 350$ nm.

Considering a silver nanosphere of radius $R = 10$ nm, $\epsilon = -2 + 0.6i$, and $\lambda_p = 350$ nm [31], for a displacement of $r_0 \approx 0.07$ nm, a strong directional scattering in the far field is observed. In Fig. 3, we plot the three-dimensional far-field scattering pattern at the displacement of $r_0 = 0.07$ nm, $r_0 = 0$ nm, and $r_0 = -0.07$ nm. A very strong dependence of the far-field scattering pattern on the displacement confirms the essential role of magnetic dipole scattering b_1 even for the case of a small metallic nanosphere. For the nanosphere case, the same radius would yield a smaller displacement at the maximum asymmetry (0.07 nm compared with the 0.1 nm case for the cylinder). However, because the nanosphere scatters less efficiently than the nanowire, the metallic nanowire is preferred for the experimental implementation. It is interesting to mention the observed anomalous scattering for the low dissipative materials and the switching of the far-field scattering around electric quadrupole resonances [37–40]. However, in our system, we do not require the material to have low dissipation. More importantly, our scheme is based on the interference between the electric dipolar contribution and the magnetic dipolar contribution, while the latter contribution is generally neglected.

In conclusion, we have shown that the usually neglected magnetic response from a metallic nanowire can be used to develop an ultrasensitive method for the measurement of deflection. For a radius much smaller than the wavelength, the metallic nanowire working at the LPR wavelength yields the maximum sensitivity to small deflections, which is, in particular, much higher than what can be achieved with the purely HRI dielectric counterpart. The essential role of magnetic dipole scattering also exists in the 3D metallic nanosphere case. It is expected that the rethinking of the role of magnetic dipole scattering in a metallic nanowire and in a metallic nanosphere would provide new guidelines for the development of sensors that are important in various metrology and superresolution applications and also yields interesting physics involving interactions between the magnetic component of light and matter.

The authors would like to thank Lei Wei for inspiring discussions and Sander Konijnenberg for reading of the manuscript.

*z.xi@tudelft.nl

[1] M. Quinten, *Optical Properties of Nanoparticle Systems: Mie and Beyond* (John Wiley & Sons, New York, 2010).

[2] C. F. Bohren and D. R. Huffman, *Absorption and Scattering of Light by Small Particles* (John Wiley & Sons, New York, 2008).

[3] H. van de Hulst, *Light Scattering by Small Particles* (Dover, New York, 1981).

[4] M. Burresi, D. Van Oosten, T. Kampfrath, H. Schoenmaker, R. Heideman, A. Leinse, and L. Kuipers, Science **326**, 550 (2009).

[5] K. Vynck, D. Felbacq, E. Centeno, A. I. Căbuz, D. Cassagne, and B. Guizal, Phys. Rev. Lett. **102**, 133901 (2009).

[6] S. Vignolini, F. Intonti, F. Riboli, L. Balet, L. H. Li, M. Francardi, A. Gerardino, A. Fiore, D. S. Wiersma, and M. Gurioli, Phys. Rev. Lett. **105**, 123902 (2010).

[7] S. Karaveli and R. Zia, Phys. Rev. Lett. **106**, 193004 (2011).

[8] H. Kihm, S. Koo, Q. Kim, K. Bao, J. Kihm, W. Bak, S. Eah, C. Lienau, H. Kim, P. Nordlander *et al.*, Nat. Commun. **2**, 451 (2011).

[9] A. Asenjo-Garcia, A. Manjavacas, V. Myroshnychenko, and F. G. de Abajo, Opt. Express **20**, 28142 (2012).

[10] S.-Y. Lee, I.-M. Lee, J. Park, S. Oh, W. Lee, K.-Y. Kim, and B. Lee, Phys. Rev. Lett. **108**, 213907 (2012).

[11] N. Rotenberg, M. Spasenović, T. L. Krijger, B. le Feber, F. J. Garcia de Abajo, and L. Kuipers, Phys. Rev. Lett. **108**, 127402 (2012).

[12] J.-M. Yi, A. Cuche, F. de León-Pérez, A. Degiron, E. Laux, E. Devaux, C. Genet, J. Alegret, L. Martín-Moreno, and T. W. Ebbesen, Phys. Rev. Lett. **109**, 023901 (2012).

[13] S. M. Hein and H. Giessen, Phys. Rev. Lett. **111**, 026803 (2013).

[14] N. Rotenberg, T. L. Krijger, B. le Feber, M. Spasenović, F. J. Garcia de Abajo, and L. Kuipers, Phys. Rev. B **88**, 241408 (2013).

[15] L. Aigouy, A. Cazé, P. Gredin, M. Mortier, and R. Carminati, Phys. Rev. Lett. **113**, 076101 (2014).

[16] T. Coenen, F. B. Arango, A. F. Koenderink, and A. Polman, Nat. Commun. **5**, 3250 (2014).

[17] N. Rotenberg and L. Kuipers, Nat. Photonics **8**, 919 (2014).

[18] M. Kasperczyk, S. Person, D. Ananias, L. D. Carlos, and L. Novotny, Phys. Rev. Lett. **114**, 163903 (2015).

[19] E. Gil-Santos, D. Ramos, J. Martínez, M. Fernández-Regúlez, R. García, Á. San Paulo, M. Calleja, and J. Tamayo, Nat. Nanotechnol. **5**, 641 (2010).

[20] B. Sanii and P. D. Ashby, Phys. Rev. Lett. **104**, 147203 (2010).

[21] A. Gloppe, P. Verlot, E. Dupont-Ferrier, A. Siria, P. Poncharal, G. Bachelier, P. Vincent, and O. Arcizet, Nat. Nanotechnol. **9**, 920 (2014).

[22] X. Ma, Y. Zhu, S. Kim, Q. Liu, P. Byrley, Y. Wei, J. Zhang, K. Jiang, S. Fan, R. Yan *et al.*, Nano Lett. **16**, 6896 (2016).

[23] L. M. de Lépinay, B. Pigeau, B. Besga, P. Vincent, P. Poncharal, and O. Arcizet, Nat. Nanotechnol. **12**, 156 (2017).

[24] N. Rossi, F. R. Braakman, D. Cadeddu, D. Vasyukov, G. Ttncoglu, A. Fontcuberta i Morral, and M. Poggio, Nat. Nanotechnol. **12**, 150 (2017).

[25] M. Kerker, D.-S. Wang, and C. Giles, J. Opt. Soc. Am. **73**, 765 (1983).

[26] M. Neugebauer, P. Woźniak, A. Bag, G. Leuchs, and P. Banzer, Nat. Commun. **7**, 11286 (2016).

[27] Z. Xi, L. Wei, A. J. L. Adam, H. P. Urbach, and L. Du, Phys. Rev. Lett. **117**, 113903 (2016).

[28] A. Hemmerich and T. W. Hänsch, Phys. Rev. Lett. **68**, 1492 (1992).

[29] S. Albaladejo, M. I. Marqués, M. Laroche, and J. J. Sáenz, Phys. Rev. Lett. **102**, 113602 (2009).

[30] J. Barry, D. McCarron, E. Norrgard, M. Steinecker, and D. DeMille, Nature (London) **512**, 286 (2014).

[31] E. D. Palik, *Handbook of Optical Constants of Solids* (Academic Press, New York, 1998), Vol. 3.

[32] E. Kallos, I. Chremmos, and V. Yannopapas, Phys. Rev. B **86**, 245108 (2012).

[33] See Supplemental Material at http://link.aps.org/supplemental/10.1103/PhysRevLett.119.053902 for further details, which includes Refs. [1,2,34].

[34] M. Z. Alam, I. De Leon, and R. W. Boyd, Science **352**, 795 (2016).

[35] R. Hillenbrand, T. Taubner, and F. Keilmann, Nature (London) **418**, 159 (2002).

[36] L. Wei, Z. Xi, N. Bhattacharya, and H. P. Urbach, Optica **3**, 799 (2016).

[37] M. I. Tribelsky and B. S. Luk'yanchuk, Phys. Rev. Lett. **97**, 263902 (2006).

[38] M. I. Tribelsky, S. Flach, A. E. Miroshnichenko, A. V. Gorbach, and Y. S. Kivshar, Phys. Rev. Lett. **100**, 043903 (2008).

[39] A. E. Miroshnichenko, S. Flach, and Y. S. Kivshar, Rev. Mod. Phys. **82**, 2257 (2010).

[40] B. Luk'yanchuk, N. I. Zheludev, S. A. Maier, N. J. Halas, P. Nordlander, H. Giessen, and C. T. Chong, Nat. Mater. **9**, 707 (2010).

[41] M. Piliarik and V. Sandoghdar, Nat. Commun. **5**, 4495 (2014).